International Journal of Mechanical and Production
Engineering Research and Development (IJMPERD)
ISSN (P): 2249-6890; ISSN (E): 2249-8001
Vol. 8, Issue 4, Aug 2018, 1-8

MULTI-DIMENSIONAL FLOW ANALYSIS OF GOLDBERG FALCON REMOTE CONTROLLED AIRCRAFT WING

P. HANUMA[1], M. SNIGDHA[2], G. SWATHI[3] & B. ALEKYA[4]

[1,2,3] Assistant Professor, Department of Aeronautical Engineering, Institute of Aeronautical Engineering, Dundigal, Hyderabad, Telangana, India

[4]Department of Aeronautical Engineering, MLR Institute of Technology, Dundigal, Hyderabad, Telangana, India

ABSTRACT

The wing is very important part of the airplane assists in producing the lift required for the flight. This work simulates the flow over a three-dimensional design of the falcon wing and tries to analyze the streamline pattern over the wing. This particular design of the wing is used in Carl Goldberg Falcon 56 Mk II R/C power plane. Flow properties around the wing as well on the wing surface body have been analyzed by using K-epsilon turbulence model. Flow patterns over the cross-section of the wing were analyzed and clearly plotted by using different contours of pressure temperatures and velocities.

KEYWORDS: CFD Analysis of the Wing, Aerofoil & 3D Wing Analysis

Received: Apr 18, 2018; **Accepted**: May 05, 2018; **Published:** Jun 22, 2018; **Paper Id**: IJMPERDAUG20181

Original Article

INTRODUCTION

This current paper deals with the CFD analysis of the wing of an RC plane. Flow analysis for Goldberg falcon plane had been done. Falcon 56 is a propeller-driven RC plane which has a wingspan of 1422 mm and weighs almost 2495 Kg. The wing design is based on a semi-symmetrical aerofoil with a tricycle style of the landing gear. Its length is approximately 1206 mm as shown in figure 1. [8]

Developments on the flow over a 3D wing with vortex separation on the leading edge had been demonstrated by F. T Johnson et.al. They compared both the computational and experimental results to make an estimation of the vortex formation criteria. [1]

Figure 1: Carl Goldberg Falcon 56 Mk II R/C Power Plane [10]

J. Johnasen and team came out with a method of taking out airfoil characteristics from three dimensional CFD data. They used wind speed and angle of attack to compute the coefficient of lift drag and other forces acting on the blade. [2]

M. Snigdha and team had simulated the 3D flow over a wing-body junction by varying different junction designs. Their main concentration was to visualize the flow over the junction of wing and horseshoe vortex formation. G. Swathi Ett.al has simulated a three-dimensional flow over spike nozzle at various pressure conditions. [3], [4], [5]. A. M Morris et. al presented a novel domain element shape parameterization technique for CFD-based shape optimization. Their method is to achieve two basic criteria's one is to provide a generic 'wrap-around' optimization tool that is independent of both flow solver and grid generation package and the second one is to provide a method that allows high-fidelity aerodynamic optimization of 2D and 3D bodies with a low number of design variables. Results are presented for two-dimensional airfoil inverse design and drag optimization problems. Inverse design results demonstrate that a large proportion of the design space is feasible with a relatively low number of design variables using the domain element parameterization. [6] D. J Poole and team worked on the use of proper orthogonal decomposition to derive airfoil design variables. They also demonstrated an efficient and reduced set of orthogonal design variables. They highlighted the importance of the application of a constrained global optimizer to aerodynamic optimization. At last, they have shown that as few as six variables are required for airfoil optimization.

WING DESIGN, GRID GENERATION, AND MATHEMATICAL MODELLING

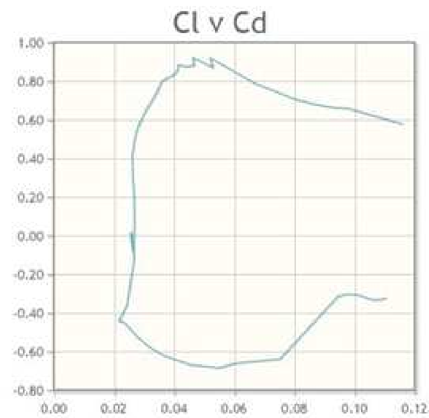

Figure 2: CL Vs CD Plot

Figure 3: CL Vs Alpha Plot

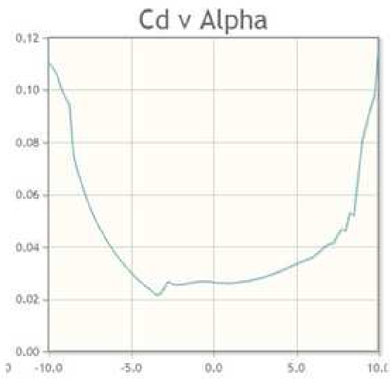

Figure 4: CD Vs Alpha Plot

Table 1: Clearly Shows the Coordinates used to Generate the Falcon RC Planes Airfoil

Point No	X Coordinate	Y Coordinate
1.	1	0.001341
2.	0.99754	0.002771
3.	0.9907	0.00563
4.	0.98037	0.008009
5.	0.96698	0.009693
6.	0.95044	0.011476
7.	0.93064	0.014067
8.	0.53099	0.06816
9.	0.49265	0.072038
10.	0.45435	0.075505
11.	0.41638	0.078438
12.	0.37887	0.080744
13.	0.34204	0.082344
14.	0.30609	0.083164
15.	0.2712	0.083128
16.	0.2376	0.082152
17.	0.20549	0.080166
18.	0.00548	0.011706
19.	0.00098	0.004376
20.	0.45435	-0.0519
21.	0.49265	-0.05041
22.	0.53099	-0.04857
23.	0.90775	-0.01528
24.	0.93064	-0.0127
25.	0.95044	-0.01063
26.	0.96698	-0.00921
27.	0.98037	-0.00799
28.	0.9907	-0.00586
29.	0.99754	-0.00301
30.	1	-0.00155

Table 1 Airfoil Coordinates[9]

Plots were created for different aerodynamic forces as shown in figure 2, 3, 4. Initially the airfoil has been designed by using the coordinates and then it has been extruded to create the wing. After that fluid domain was created around the wing followed by generating the grid file as shown in figure 5. The grid file has 419798 nodes and 2322602 elements with tetrahedral dominance.

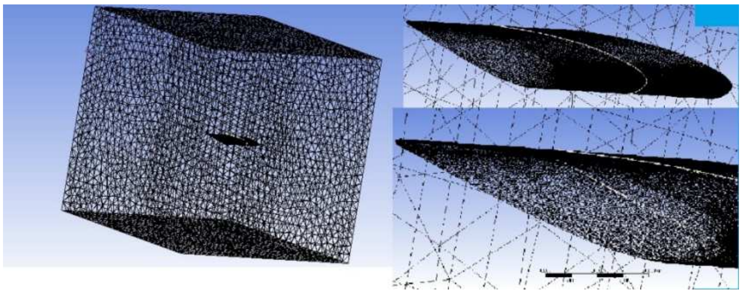

Figure 5: Meshed Fluid Domain the Wing

Continuity, momentum, and energy equations are the basic mathematical statements of three fundamental physical principles upon which all of fluid dynamics is based i.e. mass is conserved, F = ma (Newton's second law); energy is conserved. Given below are the lists of governing equations which solve the fluid domain problem.

Continuity Equation

$D\rho/Dt + \rho\, \Delta .V = 0$

Momentum Equation

$\rho\,(Du/Dt) = -(\partial p/\partial x) + (\partial \tau_{xx}/\partial x) + (\partial \tau_{yx}/\partial y) + (\partial \tau_{zx}/\partial z) + \rho\, f_x$

Energy Equation

$\rho\,(De/Dt) = \rho\, q^{dot} + \partial/\partial x\,(k\,\partial T/\partial x) + \partial/\partial y\,(k\,\partial T/\partial y) + \partial/\partial z\,(k\,\partial T/\partial z) - p\,(\partial u/\partial x + \partial v/\partial y + \partial w/\partial z) + \tau_{xx}(\partial u/\partial x) + \tau_{yx}(\partial u/\partial y) + \tau_{zx}(\partial u/\partial z) + \tau_{yx}(\partial v/\partial x) + \tau_{yy}(\partial v/\partial y) + \tau_{zy}(\partial v/\partial z) + \tau_{xz}(\partial w/\partial x) + \tau_{yz}(\partial w/\partial y) + \tau_{zz}(\partial w/\partial z)$

Navier Strokes Equation

$\partial(\rho.u)/\partial t + \partial(\rho u^2)/\partial x + \partial(\rho uv)/\partial y + \partial(\rho uw)/\partial z = -\partial p/\partial x + \partial/\partial x\,[\lambda\, \Delta \cdot V + 2\mu\,(\partial u/\partial x)] + \partial/\partial y\,[\mu\{(\partial v/\partial x) + (\partial u/\partial y)\}] + \partial/\partial z\,[\mu\{(\partial u/\partial z) + (\partial w/\partial x)\}] + \rho\, fx$

PROBLEM DEFINITION

The wing was simulated with flow of speed 200 m/s and outlet of 3000 Pa. K- epsilon model was used to capture the turbulence phenomena. The domain surrounding the wing apart of inlet and outlet were given far field opening conditions with 3000 Pa of pressure outlet. Figure 6 clearly shows the boundary conditions taken in the problem.

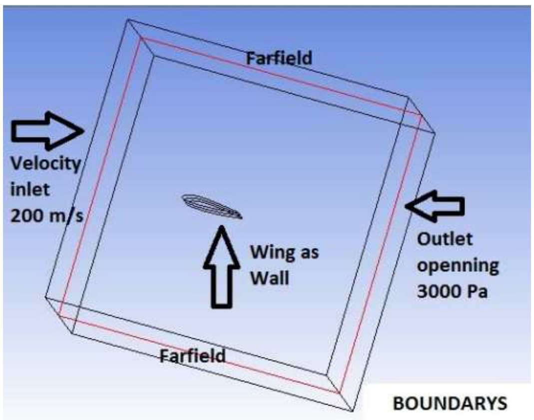

Figure 6: Boundary Conditions in the Problem

RESULTS AND DISCUSSIONS

Streamlines around and on the wing surface are clearly represented in figure 7, 8 and 9.

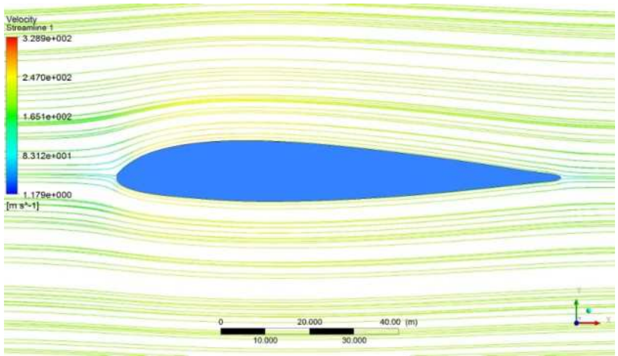

Figure 7: Velocity Streamlines around the Wings Airfoil

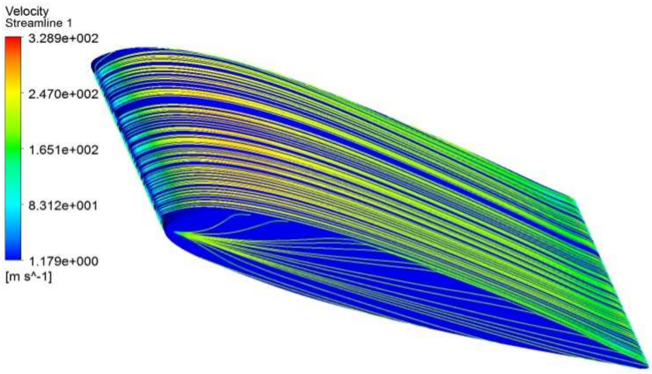

Figure 8: Velocity Streamlines on the Wing Surface

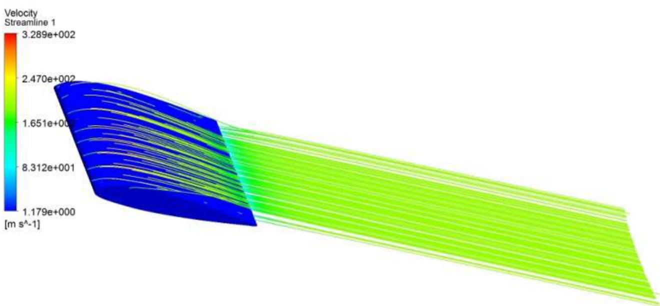

Figure 9: Velocity Streamlines Crossing the Wing Surface

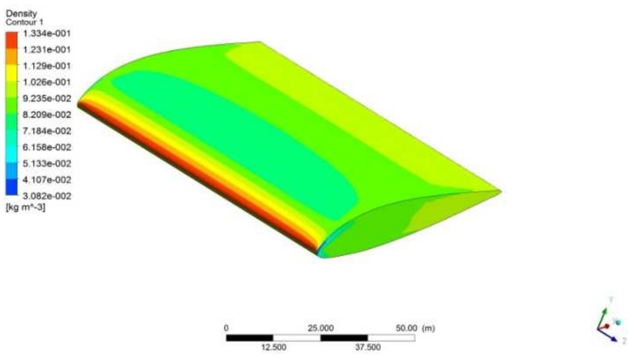

Figure 10: Density Variation over the Wing Surface

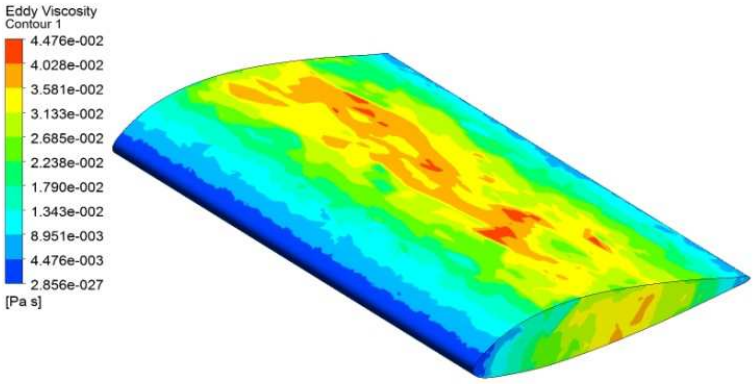

Figure 11: Variation of Eddy over the Wing Surface

Figure 12: Temperature Variation over the Wing Surface

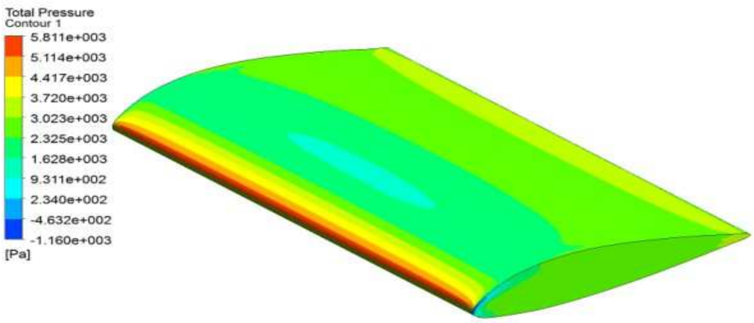

Figure 13: Total Pressure Variation over the Wing Surface

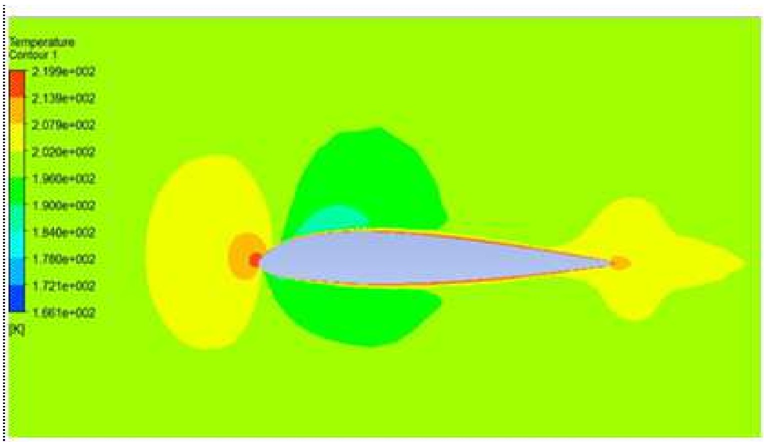

Figure 14: Temperature Contours over the Airfoil

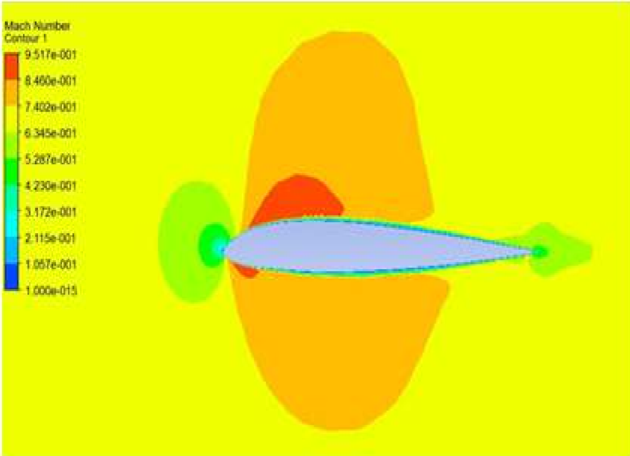

Figure 15: Mach Contours over the Airfoil

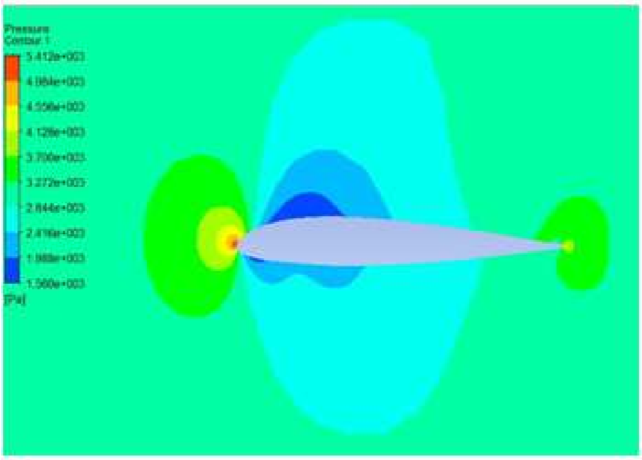

Figure 16: Pressure Contours over the Airfoil

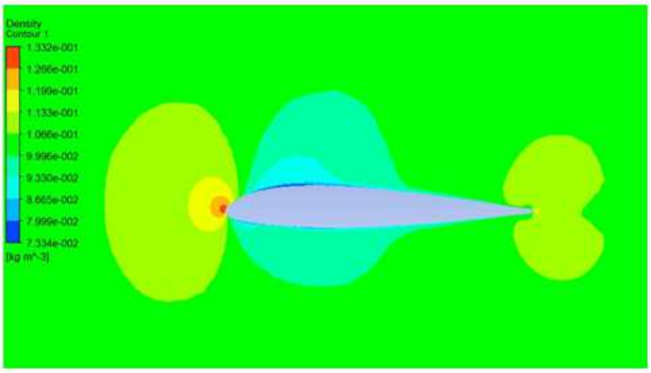

Figure 17: Density Contours over the Airfoil

Flow properties around the airfoil and on the wing have been determined. Pressure variation around the wing with temperature and density changes has been represented. In the streamlines, it could be clearly seen how the flow at the bottom of the wing is less than the top of the wing causing pressure difference for the lift to be generated.

CONCLUSIONS

- Both 2D and 3D flow analysis over the Falcon UAV have been performed.
- Variation of flow properties like Mach number, density, and temperature around the airfoil has been represented.
- Pressure-temperature and viscosity variation on the wing have been represented in 3D.
- Streamlines gave a clear idea of the pattern of the flow around and on the surface of the wing.

REFERENCES

1. *F. T. Johnson, E. N. Tinoco, P. Lu, and M. A. Epton. "Three-Dimensional Flow over Wings with Leading-Edge Vortex Separation", AIAA Journal, Vol. 18, No. 4 (1980), pp. 367-380.*
2. *Jeppe Johansen Niels N. Sorensen, "Airfoil characteristics from 3D CFD rotor computations", Wind energy, 17 November 2004 https://doi.org/10.1002/we.127.*
3. *GorleSwathi, ChagantiSatyaSandeep, MandapudiSnigdha, GudikandulaSravanthi and D. Govardhan," Three Dimensional Computational Flow Simulation of Truncated Aerospike Nozzle Considering Different Plug Lengths," Indian Journal of Science and Technology, Vol 10(14), DOI: 10.17485/ijst/2017/v10i14/111909, April 2017.*
4. *Snigdha. M, C. SatyaSandeep, Swathi. G, Shiva. U, Govardhan. D, Praveen.B, "CFD simulation of flow past wing-body junction: A 3-d approach", International Journal of Mechanical and Production Engineering Research and Development (IJMPERD), ISSN (P): 2249-6890; ISSN (E): 2249-8001Vol. 7, Issue 4, Aug 2017, 341-350.*
5. *C. Satya Sandeep, U. Shiva Prasad, R. Suresh, A. Nathan, G. Sravanthi. G, and D. Govardhan. D, " Design and analysis of submarine radome," American Institute of Physics, AIP Conference Proceedings 1859, 020025 (2017); DOI: 10.1063/1.4990178.*
6. *A. M. Morris C. B. Allen T. C. S. Rendall, "CFD-based optimization of aerofoils using radial basis functions for domain element parameterization and mesh deformation", International journal for numerical methods in fluids, 28 March 2008 https://doi.org/10.1002/fld.1769.*
7. *D. J. Poole, C. B. Allen, T. C. S. Rendall, "High-fidelity aerodynamic shape optimization using efficient orthogonal modal design variables with a constrained global optimizer", Computers & Fluids, Volume 143, 17 January 2017, Pages 1-15.*
8. *http://www.rcuniverse.com/magazine/article_display.cfm?article_id=997.*
9. *http://airfoiltools.com/airfoil/details?airfoil=falcon-il.*
10. *http://temac.ca/smf/index.php?topic=3638.0.*